

Journal of Visualized Experiments

Nuclei isolation and super resolution structured illumination microscopy for examining nucleoporin alterations in human neurodegeneration --Manuscript Draft--

Article Type:	Invited Methods Collection - JoVE Produced Video
Manuscript Number:	JoVE62789R1
Full Title:	Nuclei isolation and super resolution structured illumination microscopy for examining nucleoporin alterations in human neurodegeneration
Corresponding Author:	Alyssa Coyne Johns Hopkins University School of Medicine Baltimore, MD UNITED STATES
Corresponding Author's Institution:	Johns Hopkins University School of Medicine
Corresponding Author E-Mail:	acoyne3@jhmi.edu
Order of Authors:	Alyssa Coyne Jeffrey Rothstein
Additional Information:	
Question	Response
Please specify the section of the submitted manuscript.	Neuroscience
Please indicate whether this article will be Standard Access or Open Access.	Standard Access (\$1400)
Please indicate the city, state/province, and country where this article will be filmed . Please do not use abbreviations.	Baltimore, MD, USA
Please confirm that you have read and agree to the terms and conditions of the author license agreement that applies below:	I agree to the Author License Agreement
Please provide any comments to the journal here.	

TITLE:

Nuclei Isolation and Super-Resolution Structured Illumination Microscopy for Examining Nucleoporin Alterations in Human Neurodegeneration

AUTHORS AND AFFILIATIONS:

Alyssa N. Coyne^{1,2*}, Jeffrey D. Rothstein^{1,2*}

¹Brain Science Institute, Johns Hopkins University School of Medicine, Baltimore MD 21205

²Department of Neurology, Johns Hopkins University School of Medicine, Baltimore MD 21205

E-mail addresses of co-authors:

Alyssa N. Coyne (aoyne3@jhmi.edu)

Jeffrey D. Rothstein (jrothstein@jhmi.edu)

*Corresponding authors:

Alyssa N. Coyne (aoyne3@jhmi.edu)

Jeffrey D. Rothstein (jrothstein@jhmi.edu)

KEYWORDS:

nuclei, nuclear pore complex, nucleoporins, iPSNs, postmortem tissue, structured illumination microscopy, super-resolution microscopy, neurodegeneration

SUMMARY:

This protocol describes an optimized workflow for nuclei isolation and super-resolution structured illumination microscopy to evaluate individual nucleoporins within the nucleoplasm and NPCs in induced pluripotent stem cell derived neurons and postmortem human tissues.

ABSTRACT:

The nuclear pore complex (NPC) is a complex macromolecular structure comprising multiple copies of ~30 different nucleoporin proteins (Nups). Collectively, these Nups function to regulate genome organization, gene expression, and nucleocytoplasmic transport (NCT). Recently, defects in NCT and alterations to specific Nups have been identified as early and prominent pathologies in multiple neurodegenerative diseases, including Amyotrophic Lateral Sclerosis (ALS), Alzheimer's Disease (AD)/Frontotemporal Dementia (FTD), and Huntington's Disease (HD). Advances in both light and electron microscopy allow for a thorough examination of sub-cellular structures, including the NPC and its Nup constituents, with increased precision and resolution. Of the commonly used techniques, super-resolution structured illumination microscopy (SIM) affords the unparalleled opportunity to study the localization and expression of individual Nups using conventional antibody-based labeling strategies. Isolation of nuclei prior to SIM enables the visualization of individual Nup proteins within the NPC and nucleoplasm in fully and accurately reconstructed 3D space. This protocol describes a procedure for nuclei isolation and SIM to evaluate Nup expression and distribution in human iPSC-derived CNS cells and postmortem tissues.

INTRODUCTION:

The prevalence of age-related neurodegenerative diseases is increasing as the population ages¹. While the genetic underpinnings and pathologic hallmarks are well characterized, the precise molecular events leading to neuronal injury remain poorly understood^{2–12}. Recently, a G₄C₂ hexanucleotide repeat expansion in the first intron of the C9orf72 gene was identified as the most common genetic cause of the related neurodegenerative diseases Amyotrophic Lateral Sclerosis (ALS) and Frontotemporal Dementia (FTD)^{13,14}. Several studies now support a central role for disruptions in the nuclear transport machinery, including nuclear pore complexes (NPCs) and nuclear transport receptors (NTRs, karyopherins) as being causative of C9orf72 ALS^{15,16}. In non-dividing cells within the rat brain, scaffold nucleoporins (Nups) are extremely long-lived. As a result, alterations in NPCs and NCT have been reported during aging^{17–20}. Moreover, some nucleoporins or transportins, when mutated, are linked to specific neurological diseases^{21,22}. For example, mutations in Nup62 have been linked to Infantile Bilateral Striatal Necrosis (IBSN), a neurological disorder affecting the caudate nucleus and putamen²³; mutations in Gle1 have been implicated in the fetal motor neuron disease Human Lethal Congenital Contracture Syndrome-1 (LCCS1)²⁴; and mutations in Aladin are causative of Triple-A Syndrome²⁵. Alterations in functional NCT are exacerbated in age-related neurodegenerative diseases such as ALS, Huntington's Disease (HD), and Alzheimer's Disease (AD)^{16,26–31}. In addition, specific Nups and NTRs have been reported as modifiers of C9orf72 mediated toxicity in the *Drosophila* eye²⁸ or biochemically modify the aggregation state of disease-linked proteins such as FUS and tau^{27,32–34}. Collectively, these early studies suggest that altered NCT may be a primary and early pathological feature of ALS and FTD. Studies in overexpression-based model system have suggested that mislocalization of specific Nups and karyopherins may impact NCT^{16,35–38}. However, these pathology studies do not actually link cytoplasmic accumulations of NPC proteins to defects in the structure or function of the NPC. For example, this pathology may simply reflect the dysregulation of cytoplasmic pools of Nup proteins with little impact on NPC composition and function. In contrast, a recent study employing super resolution structured illumination microscopy (SIM) demonstrates the emergence of a significant injury to the NPC itself characterized by reduction in specific Nup levels within the nucleoplasm and NPCs of human C9orf72 ALS/FTD neurons ultimately leading to altered NPC function as an early initiating event in pathogenic disease cascades¹⁵.

The passage of macromolecules between the nucleus and cytoplasm is critically governed by the nuclear pore complex (NPC). The NPC is a large macromolecular complex embedded in the nuclear envelope comprising multiple copies of 30 nucleoporin proteins (Nups)^{39–41}. Although Nup stoichiometry varies among cell types^{42–44}, maintenance of overall NPC composition is critical for NCT, genome organization, and overall cellular viability^{39,41,45,46}. As a result, altered NPC composition and subsequent defects in functional transport are likely to impact a myriad of downstream cellular functions. The Nup constituents of the NPC are highly organized into multiple subcomplexes, including the cytoplasmic ring and filaments, central channel, outer ring, inner ring, transmembrane ring, and nuclear basket. Collectively, scaffold Nups of the inner, outer, and transmembrane rings anchor NPCs within the nuclear envelope and provide anchor points for Nups of the cytoplasmic ring, central channel, and nuclear basket. While small molecules (<40–60 kD) can passively diffuse through the NPC, the active transport of larger cargoes is facilitated by interactions between nuclear transport receptors (NTRs, karyopherins)

and the FG Nups of the cytoplasmic filaments, central channel, and nuclear basket^{39–41,45}. Also, a handful of Nups can additionally function outside of the NPC, within the nucleoplasm, to regulate gene expression^{46,47}.

Given that the lateral dimension of a single human NPC is approximately 100–120 nm⁴⁰, standard widefield or confocal microscopy is insufficient to resolve individual NPCs⁴⁸. Electron microscopy (EM) techniques such as TEM or SEM are often used to evaluate the overall structure of NPCs^{39,40}. Despite the advantages of these techniques for resolving NPC ultrastructure, they are less commonly used to evaluate the presence of individual Nup proteins within the NPC. The technical limitations of combining antibody or tag-based labeling with these state-of-the-art technologies, TEM and SEM, do not always allow for an accurate and reliable assessment of individual Nups themselves within NPCs or the nucleoplasm. Further, these techniques can be technically challenging and are not yet widely accessible to all researchers. However, recent advances in light and fluorescence microscopy have increased the accessibility of super-resolution imaging technologies. Specifically, SIM affords the unparalleled opportunity to image individual Nups with a resolution that approaches the lateral dimensions of one human NPC^{40,48–51}. In contrast to other super-resolution approaches such as stochastic optical reconstruction microscopy (STORM) and stimulated emission depletion (STED), SIM is compatible with conventional antibody-based immunostaining⁴⁹. Thus, SIM allows for a comprehensive analysis of all Nups for which a specific anti-Nup antibody is available. The ability to sample and image multiple different Nups in the same preparation provides significant advantages to other imaging methods when surveying the many proteins that comprise the NPC. The following procedure details an optimized protocol for evaluating individual Nup components of the NPC using nuclei isolated from induced pluripotent stem cell (iPSC) derived neurons (iPSNs) and postmortem human central nervous system (CNS) tissues.

PROTOCOL:

All blood samples for iPSC generation and autopsied tissue collections are approved by Johns Hopkins IRB with Johns Hopkins ethics oversight. All patient information is HIPPA compliant. The following protocol adheres to all Johns Hopkins biosafety procedures.

1. Preparation of slides for immunostaining and imaging

1.1 Position a positively charged glass microscope slide in an empty cytofunnel and draw a circle with a hydrophobic barrier pen to outline an area to deposit the nuclei.

1.2 Add 50 µL of 1 mg/mL collagen solution (diluted in 1x PBS) to the center of the circle drawn in step 1.1 and incubate at room temperature for 5 min.

1.3 Aspirate the collagen solution and let the slides air dry at room temperature for about 1 h.

2. Preparation of lysis buffer and sucrose gradients

2.1 Prepare the lysis buffer and sucrose gradient solutions according to the nuclei isolation kit protocol.

2.1.1 For each sample, prepare a 50 mL conical tube of lysis buffer by combining 11 mL of the supplied lysis buffer, 110 μ L of the supplied 10% Triton X-100 solution, and 11 μ L of freshly prepared or thawed 1 M DTT (Dithiothreitol).

2.1.2 For each sample, use a 50 mL conical tube to prepare a 1.85 M sucrose cushion solution by combining 27.75 mL of the supplied 2 M sucrose cushion solution, 2.25 mL of the supplied sucrose cushion buffer, and 30 μ L of freshly prepared or thawed 1 M DTT.

NOTE: A 1.85 M sucrose cushion solution is optimal for iPSNs and postmortem human CNS tissue, but adjust it for other cell types or tissue samples. Additional details for HEK293 cells, iPSC-derived astrocytes, and enrichment of oligodendrocyte nuclei from postmortem CNS tissues have recently been published¹⁵.

2.2 Gently mix lysis buffer and sucrose cushion solutions by inverting conical tubes and store it on ice.

3. Lysis of iPSNs and postmortem human CNS tissue

3.1 Before proceeding with the lysis, place the ultracentrifuge rotor (without sample holders) in the ultracentrifuge and allow it to pre-cool to 4 °C.

3.2 Lysis of iPSNs.

NOTE: Lysis protocols differ for iPSNs and postmortem human CNS tissue. Follow the protocol for the sample type specified below (step 3.2: iPSNs, step 3.3: postmortem human CNS tissue).

3.2.1 Remove the iPSNs from the incubator and aspirate the media. Rinse briefly with 1x PBS and add the lysis buffer directly to the well or plate.

NOTE: Take care to adequately rinse iPSNs with a sufficient quantity of 1x PBS to remove debris and dead cells. The volume of lysis buffer to be added to iPSN plates will vary. Please refer to **Table 1**. Ensure that the starting material is >2.5 million iPSNs.

3.2.2 Scrape the iPSNs with a cell scraper and transfer them to the remaining lysis buffer in the 50 mL conical tube.

3.2.3 Cap each conical tube and vortex the samples for 20 s to facilitate iPSN lysis.

3.2.4 Let the samples sit on ice for 1–2 min before proceeding.

3.3 Lysis of postmortem human CNS tissues.

3.3.1 Weigh out ~100 mg of frozen postmortem human CNS tissue by cutting with a razor blade in a Petri dish placed on a bed of dry ice. Be sure to work on a surface surrounded by disposable pads to avoid local tissue contamination. Pay attention to specific gray matter versus white matter dissections (e.g., cortical mantle versus underlying white matter) visible at the time of tissue dissection.

NOTE: Wear the appropriate PPE, including eye protective wear and gloves when handling frozen postmortem human tissue samples. This step can also be completed ahead of time and tissue aliquots stored at -80 °C. 50 mg is a sufficient quantity for nuclei isolation. However, more than 100 mg tissue often yields incomplete isolation of nuclei, as evidenced by the presence of intact cytoplasm surrounding some nuclei.

3.3.2 Prepare the Dounce homogenizer by cleaning and thoroughly rinsing with distilled water. Chill the homogenizer by placing it on ice.

3.3.3 Add 100 mg of tissue to freshly cleaned, rinsed, and chilled (on ice) Dounce homogenizer containing 2 mL of the prepared lysis buffer.

3.3.4 Homogenize in Dounce homogenizer using the standard procedure on ice.

NOTE: Typically, 10–20 strokes per pestle is sufficient to move through the sample without resistance.

3.3.5 Transfer 2 mL of postmortem human brain homogenate to the remaining 9 mL of lysis buffer in conical tubes.

3.3.6 Vortex vigorously for 30 s and let it sit on ice for 5 min to facilitate lysis.

4. Isolation of nuclei from iPSNs and postmortem human CNS tissue

4.1 Layer 10 mL of 1.85 M sucrose cushion solution (made in step 2.1.2) at the bottom of an ultracentrifuge tube and add 18 mL of 1.85 M sucrose cushion solution to each lysate.

4.2 Gently mix the lysate/sucrose cushion solution (combined in step 4.1) by inverting the 50 mL conical tube.

4.3 Slowly add 28 mL of lysate/sucrose cushion solution mix to the top of the 10 mL of 1.85 M sucrose cushion solution in the ultracentrifuge tube (from step 4.1).

NOTE: There is a total of 29 mL lysate/sucrose cushion solution mix in the 50 mL conical tube (steps 4.1–4.2). Leave 1 mL of this lysate/sucrose cushion solution mix in the 50 mL conical tube. This ensures accurate and consistent pipetting among all samples due to the viscosity of the sucrose cushion solution.

221
222 4.4 Place the ultracentrifuge tubes in the holders and add an additional 1.85 M sucrose cushion
223 solution (made in step 2.1.2) as needed to balance the samples.

224
225 4.5 Place the sample holders in the rotor in the chilled ultracentrifuge and spin at 30,000 x *g*, 4
226 °C for 45 min.

227
228 4.6 Remove the ultracentrifuge tubes from the sample holders and discard the supernatants.
229 Nuclei will be visible as pellets on the bottom sides of the ultracentrifuge tube.

230
231 4.7 Resuspend the nuclei pellets in 1 mL of the supplied nuclei storage buffer by vortexing and
232 transfer to a microcentrifuge tube.

233
234 4.8 Centrifuge the microcentrifuge tubes at 2,500 x *g*, 4 °C for 5 min.

235
236 4.9 Remove the supernatant and resuspend the nuclei by vortexing in fresh 1 mL of the supplied
237 nuclei storage buffer.

238
239 4.10 Proceed with immunostaining or store the nuclei at -80 °C.

240
241 NOTE: Nuclei can be stored at -80 °C for up to 6 months and be subjected to two freeze/thaw
242 cycles before structural integrity is compromised.

243 244 **5. Immunostaining of the isolated nuclei**

245
246 5.1 Take a 10 µL aliquot of the nuclei suspension and count using a hemacytometer or an
247 automated cell counter.

248
249 5.2 Assemble the prepared slides (from step 1.3) into the cytofunnels.

250
251 5.3 To each cytofunnel, layer 200 µL of fresh nuclei storage buffer and ~100,000 nuclei.

252
253 5.4 Gently spin the nuclei onto the slides by placing the cytofunnels into a cytospin and
254 centrifuging for 3 min at 100 x *g*.

255
256 5.5 Unclip the cytofunnels and immediately add ~100 µL of 4% PFA (paraformaldehyde) to the
257 slides and incubate for 15 min at room temperature.

258
259 NOTE: Nuclei can also be fixed with methanol. Use fixation method appropriate for each
260 antibody. If using methanol, skip the permeabilization step (5.7). Cytofunnels are single-use;
261 discard them at this point.

262
263 5.6 Wash the nuclei 3x for 5 min with 1x PBS.

264

265 5.7 Permeabilize the nuclei with 0.1% Triton X-100 in 1x PBS for 10 min at room temperature.

266
267 5.8 Block the nuclei in block solution (10% goat or donkey serum in 1x PBS) for 30 min at room
268 temperature.

269
270 5.9 Incubate the nuclei with primary antibodies diluted in block solution overnight at 4 °C.

271
272 5.10 Wash the nuclei 3x for 5 min with 1x PBS.

273
274 5.11 Incubate the nuclei with secondary antibodies diluted in block solution for 1 h at room
275 temperature.

276
277 NOTE: Alexa Fluor 488, 568, and 647 secondary antibodies are preferred.

278
279 5.12 Wash the nuclei 3x for 5 min with 1x PBS.

280
281 5.13 OPTIONAL: Incubate the nuclei for 5 min with DAPI or Hoechst followed by two additional 5
282 min washes with 1x PBS.

283
284 5.14 Hold a lint-free wipe at the edge of the circle containing nuclei to remove the last PBS wash
285 completely.

286
287 5.15 Add 1 drop (~10 µL) of a hard mount antifade mounting media (without DAPI) to each slide
288 and gently place high tolerance 18 mm x 18 mm square coverslips on each slide.

289
290 NOTE: When using a hard-mount media, slide sealing is not necessary if slides are imaged within
291 an appropriate time frame. Nup immunoreactivity has typically remained stable on unsealed
292 slides stored at 4 °C for ~6 months. However, the edges of the coverslip can be sealed with a thin
293 layer of nail polish if a wet-mount media is used or for prolonged storage.

294
295 5.16 Keep the slides protected from light and let them cure overnight at room temperature.

296
297 5.17 Image the nuclei can by super-resolution structured illumination microscopy (SIM).

298
299 NOTE: Zeiss, Nikon, and GE Healthcare all manufacture SIM microscopes. Follow the system-
300 specific protocols for image acquisition and processing. Use imaging parameters (laser power,
301 filter sets, exposure time) appropriate for each Nup and fluorophore. When imaging, avoid edges
302 of the circle (from step 1.1) as these nuclei are typically flattened and spread out as a result of
303 the centrifugation step (5.4). Fully deconvolved and processed images can be subjected to a
304 number of analyses, including spot detection and volume measurements using standard 3D
305 analysis modules in FIJI or Imaris image analytics software. Additional details on analysis methods
306 have been recently published¹⁵.

307
308 **REPRESENTATIVE RESULTS:**

To examine the NPC and nucleoplasmic distribution and expression of POM121 in human neuronal nuclei control, and C9orf72 iPSNs were differentiated as previously described¹⁵. Postmortem human motor cortex and day 32 iPSNs were lysed and subjected to nuclei isolation and immunostaining as described above. NeuN positive isolated nuclei were imaged by super-resolution structured illumination microscopy (SIM) using a super-resolution structured illumination microscope (Zeiss) and processed using default structured illumination deconvolution parameters as previously described¹⁵ (see also **Figure 1** for workflow). Images were acquired using a 63x oil immersion objective, 1x magnification, an HR Diode 448 laser at 1% power, exposure time of 100 ms, BP495–550/LP750 emission filter, 110 nm thick z sections, and 5 grid rotations. As shown in 3D maximum intensity projections in **Figure 2**, individual POM121 spots were resolved in both iPSN and postmortem neuronal nuclei. These images were subsequently subjected to spot detection using the 3D suite plugin in FIJI or Imaris as previously described¹⁵. Consistent with prior analyses¹⁵, this methodology was sufficient to detect a substantial decrease in the number of POM121 spots in C9orf72 iPSN and postmortem motor cortex nuclei compared to controls (**Figure 2**).

FIGURE AND TABLE LEGENDS:

Figure 1: Schematic representation of nuclei isolation, immunofluorescent staining, super-resolution imaging, and analysis workflow.

Figure 2: Representative structured illumination microscopy (SIM) images and quantification. (A–B) Maximum intensity projection SIM images and quantification of POM121 spots in NeuN+ nuclei isolated from control and C9orf72 iPSNs. n = 3 control and 3 C9orf72 iPSC lines, 50 nuclei per line. Student's *t*-test was used to calculate statistical significance. **** p < 0.0001. (C–D) Maximum intensity projection SIM images and quantification of POM121 spots in NeuN+ nuclei isolated from control and C9orf72 postmortem motor cortex tissue. n = 3 control and 3 C9orf72 patient cases, 50 nuclei per case. Student's *t*-test was used to calculate statistical significance. **** p < 0.0001. Scale bar = 5 μm. Statistical analyses were performed whereby the average number of spots from 50 nuclei per iPSC line were used to calculate statistical significance as previously described¹⁵.

Table 1: Lysis buffer volumes. The table contains the information of lysis buffer volume to be used for lysis of iPSNs or cultured cells grown in different culture vessels.

DISCUSSION:

Given the recent identification of NCT deficits as an early and prominent phenomenon in multiple neurodegenerative diseases^{16,27,28,30,31} there exists a critical need to thoroughly examine the mechanism by which this pathology occurs. As the NPC and its individual Nup proteins critically control functional NCT^{39,41}, an investigation of NPC composition in neurodegenerative disease models is essential. However, standard widefield and confocal microscopy techniques are insufficient to resolve individual NPCs^{40,48,49,51}. Thus, to date, analysis of Nups at the resolution of a single NPC has not been adopted as a routine experimental approach.

In recent years, super-resolution imaging technologies such as SIM have become more

accessible. These methodologies couple conventional immunofluorescence staining with advanced image processing and deconvolution to provide increased resolution sufficient to resolve an individual NPC^{40,48,49,51}. Although compatible with standard immunostaining protocol, thereby affording researchers the ability to detect any Nup for which a specific anti-Nup antibody is available at high resolution⁴⁸⁻⁵⁰, SIM does not come without its technical challenges or limitations as outlined below.

The success of any super-resolution imaging experiment is highly dependent upon sample quality. Specifically, for SIM, incomplete nuclei isolation or over lysis of samples can lead to retention of cytoplasm and cell membranes or fragmented or collapsed and shriveled nuclei, respectively. The lysis time should be adjusted, accordingly, to overcome this issue. While the protocol detailed above has been optimized for iPSCs and postmortem human CNS tissue, it is easily amended to produce high-quality nuclei from a variety of cell types and tissues. This is accomplished by adjusting the concentration of the sucrose gradient and/or sample lysis time and method. Additional details regarding sucrose gradient adjustments for HEK293 cells, iPSC-derived astrocytes, and enrichment of oligodendrocyte nuclei from postmortem human CNS tissue have been recently published¹⁵.

The process of nuclei isolation itself may disrupt the association of less stably attached Nups or nuclear transport receptors that transiently associate with the NPC. As a result, to verify the results obtained from SIM imaging of isolated nuclei, researchers should consider employing additional techniques such as immunostaining and confocal imaging of intact cells or tissues as has been previously described¹⁵. However, it is noted that routine confocal imaging of Nups does not provide the resolution to resolve individual NPC spots⁴⁸ and thus can only provide semi-quantitative information regarding overall Nup intensity. For Nups, which are also normally present within cytoplasmic pools⁵²⁻⁵⁵, western blot analyses from whole cell lysates are not recommended as a validation method for NPC composition due to contamination from Nups that may be localized to the cytoplasm. However, western blot analyses from isolated nuclei samples have been employed to validate data obtained from imaging technologies¹⁵.

The resolution of SIM images can vary among fluorophores depending on the individual point spread functions of the specific imaging system⁵¹. This should be experimentally tested by the user for each sample type before proceeding. SIM imaging is not ideal for samples with a thickness greater than 10–15 μm ^{48,51}. As a result, nuclei isolation enables imaging of the full thickness of human nuclei and therefore provides for the most accurate 3D reconstruction and quantification of Nup spots and volume. However, in instances where nucleus thickness remains >15 μm , Airy Scan imaging can be used as an alternative. Although the resolution is decreased, Airy Scan imaging is not limited by sample thickness⁵⁶.

It should also be taken into consideration that the images presented in **Figure 2** represent maximum intensity projections following 3D reconstruction of individual nuclei imaged by SIM. Therefore, in such an image, it is difficult to accurately distinguish between spots truly associated with the NPC as opposed to those within the nucleoplasm. As a result, when analyzing 3D images, it is critical to analyze and segment each z section or small series of z sections independently to

distinguish between spots associated with the nuclear envelope as opposed to the nucleoplasm. The quantifications presented in **Figure 2** represent only those spots detected along the outside faces of the analyzed nuclei. In other words, the representative quantitation indicates the number of POM121 spots associated with the nuclear envelope.

Lastly, given nuclear heterogeneity and variability^{15,42}, it is important to image and evaluate a large number of nuclei per sample regardless of the super-resolution imaging method employed.

In contrast to bulk proteomics and western blot assays, imaging methodologies provide the unparalleled opportunity to examine the distribution and expression of Nups within subsets of human CNS cells identified by specific cell types or nuclear markers (e.g., NeuN, Olig2). SIM is one of many super-resolution imaging techniques that can be employed to study the NPC and its individual Nup components^{50,57,58}. Each methodology (SIM, STORM, EM) will yield its own insights into NPC structure and composition. While SIM is capable of evaluating each Nup for which an anti-Nup antibody is available at the resolution of a single NPC, STORM is capable of resolving the octet structure of individual NPCs, and EM techniques provide a detailed view of the overall NPC structure at high resolution⁵⁰. STORM and Immuno EM approaches to evaluate individual Nups within NPCs are technically challenging. Specifically, STORM often requires the use of endogenous fluorescent tags to overcome steric hinderance provided by conventional antibody-based staining. To date, only a handful of Nups in non-neuronal cell lines have been imaged by this technology. Furthermore, conventionally STORM images NPCs on a single surface of nuclei, thus eliminating the opportunity for full 3D reconstruction of an entire nucleus to evaluate the spatial distribution and NPC heterogeneity⁵⁰. As a result, SIM is the preferred light microscopy methodology for robustly evaluating Nups within NPCs and the nucleoplasm at high resolution. A recent study used both SEM and SIM technologies to conclude that the overall NPC structure was intact, but specific Nups were reduced from the NPC and nucleoplasm of C9orf72 ALS/FTD neuronal nuclei¹⁵. This work highlights the critical importance of combining multiple high-resolution imaging approaches to yield novel insights into both NPC composition and structure as well as the strength of SIM for examining 23 individual human Nups.

ACKNOWLEDGMENTS:

Postmortem human CNS tissues were provided by the Johns Hopkins ALS Autopsy Bank and the Target ALS Postmortem Tissue Core. This work was supported by the ALSA Milton Safenowitz Postdoctoral Fellowship (ANC), as well as funding from NIH-NINDS, Department of Defense, ALS Association, Muscular Dystrophy Association, F Prime, The Robert Packard Center for ALS Research Answer ALS Program, and the Chan Zuckerberg Initiative.

DISCLOSURES:

The authors declare no competing financial interests.

REFERENCES:

1. Hou, Y. et al. Ageing as a risk factor for neurodegenerative disease. *Nature Reviews. Neurology*. **15** (10), 565–581 (2019).
2. Kim, G., Gautier, O., Tassoni-Tsuchida, E., Ma, X. R., Gitler, A. D. ALS genetics: Gains, losses,

and implications for future therapies. *Neuron*. **108** (5), 822–842 (2020).

3. Bang, J., Spina, S., Miller, B. L. Frontotemporal dementia. *Lancet*. **386** (10004), 1672–1682 (2015).

4. Blauwendraat, C., Nalls, M. A., Singleton, A. B. The genetic architecture of Parkinson's disease. *The Lancet Neurology*. **19** (2), 170–178 (2020).

5. Cacace, R., Sleegers, K., Van Broeckhoven, C. Molecular genetics of early-onset Alzheimer's disease revisited. *Alzheimer's & Dementia*. **12** (6), 733–748 (2016).

6. Di Resta, C., Ferrari, M. New molecular approaches to Alzheimer's disease. *Clinical Biochemistry*. **72**, 81–86 (2019).

7. Karch, C. M., Cruchaga, C., Goate, A. M. Alzheimer's disease genetics: from the bench to the clinic. *Neuron*. **83** (1), 11–26 (2014).

8. Kovacs, G. G. Molecular pathology of neurodegenerative diseases: principles and practice. *Journal of Clinical Pathology*. **72** (11), 725–735 (2019).

9. McColgan, P., Tabrizi, S. J. Huntington's disease: a clinical review. *European Journal of Neurology*. **25** (1), 24–34 (2018).

10. Ross, C. A., Tabrizi, S. J. Huntington's disease: from molecular pathogenesis to clinical treatment. *The Lancet. Neurology*. **10** (1), 83–98 (2011).

11. Dugger, B. N., Dickson, D. W. Pathology of neurodegenerative diseases. *Cold Spring Harbor Perspectives in Biology*. **9** (7), a028035 (2017).

12. Ross, C. A., Poirier, M. A. Protein aggregation and neurodegenerative disease. *Nature Medicine*. **10 Suppl**, S10–17 (2004).

13. DeJesus-Hernandez, M. et al. Expanded GGGGCC hexanucleotide repeat in noncoding region of C9ORF72 causes chromosome 9p-linked FTD and ALS. *Neuron*. **72** (2), 245–256 (2011).

14. Renton, A. E. et al. A hexanucleotide repeat expansion in C9ORF72 is the cause of chromosome 9p21-linked ALS-FTD. *Neuron*. **72** (2), 257–268 (2011).

15. Coyne, A. N. et al. G(4)C(2) repeat RNA initiates a POM121-mediated reduction in specific nucleoporins in C9orf72 ALS/FTD. *Neuron*. **107** (6), 1124–1140 (2020).

16. Zhang, K. et al. The C9orf72 repeat expansion disrupts nucleocytoplasmic transport. *Nature*. **525** (7567), 56–61 (2015).

17. D'Angelo, M. A., Raices, M., Panowski, S. H., Hetzer, M. W. Age-dependent deterioration of nuclear pore complexes causes a loss of nuclear integrity in postmitotic cells. *Cell*. **136** (2), 284–295 (2009).

18. Hetzer, M. W. The role of the nuclear pore complex in aging of post-mitotic cells. *Aging (Albany NY)*. **2** (2), 74–75 (2010).

19. Savas, J. N., Toyama, B. H., Xu, T., Yates, J. R., 3rd, Hetzer, M. W. Extremely long-lived nuclear pore proteins in the rat brain. *Science*. **335** (6071), 942 (2012).

20. Toyama, B. H. et al. Identification of long-lived proteins reveals exceptional stability of essential cellular structures. *Cell*. **154** (5), 971–982 (2013).

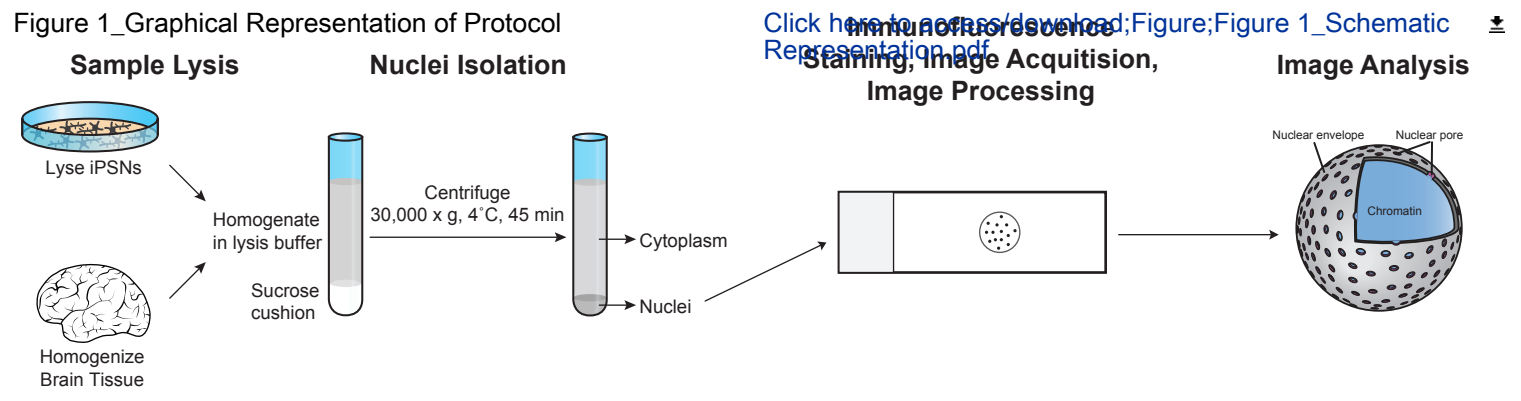
21. Nofrini, V., Di Giacomo, D., Mecucci, C. Nucleoporin genes in human diseases. *European Journal of Human Genetics*. **24** (10), 1388–1395 (2016).

22. Sakuma, S., D'Angelo, M. A. The roles of the nuclear pore complex in cellular dysfunction, aging and disease. *Seminars in Cell & Developmental Biology*. **68**, 72–84 (2017).

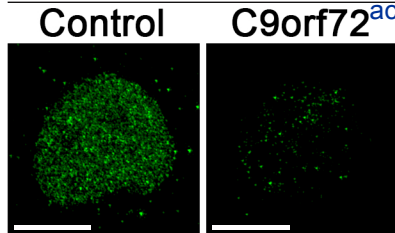
23. Basel-Vanagaite, L. et al. Mutated nup62 causes autosomal recessive infantile bilateral striatal necrosis. *Annals of Neurology*. **60** (2), 214–222 (2006).

24. Nousiainen, H. O. et al. Mutations in mRNA export mediator GLE1 result in a fetal motoneuron disease. *Nature Genetics*. **40** (2), 155–157 (2008).
25. Cronshaw, J. M., Matunis, M. J. The nuclear pore complex: disease associations and functional correlations. *Trends in Endocrinology and Metabolism*. **15** (1), 34–39 (2004).
26. Chou, C. C. et al. TDP-43 pathology disrupts nuclear pore complexes and nucleocytoplasmic transport in ALS/FTD. *Nature Neuroscience*. **21** (2), 228–239 (2018).
27. Eftekharzadeh, B. et al. Tau protein disrupts nucleocytoplasmic transport in Alzheimer's disease. *Neuron*. **99** (5), 925–940.e927 (2018).
28. Freibaum, B. D. et al. GGGGCC repeat expansion in C9orf72 compromises nucleocytoplasmic transport. *Nature*. **525** (7567), 129–133 (2015).
29. Gasset-Rosa, F. et al. Polyglutamine-expanded huntingtin exacerbates age-related disruption of nuclear integrity and nucleocytoplasmic transport. *Neuron*. **94** (1), 48–57.e44 (2017).
30. Grima, J. C. et al. Mutant huntingtin disrupts the nuclear pore complex. *Neuron*. **94** (1), 93–107.e106 (2017).
31. Jovicic, A. et al. Modifiers of C9orf72 dipeptide repeat toxicity connect nucleocytoplasmic transport defects to FTD/ALS. *Nature Neuroscience*. **18** (9), 1226–1229 (2015).
32. Guo, L. et al. Nuclear-import receptors reverse aberrant phase transitions of RNA-binding proteins with prion-like domains. *Cell*. **173** (3), 677–692.e620 (2018).
33. Hofweber, M. et al. Phase Separation of FUS Is Suppressed by Its Nuclear Import Receptor and Arginine Methylation. *Cell*. **173** (3), 706–719.e713 (2018).
34. Yoshizawa, T. et al. Nuclear Import Receptor Inhibits Phase Separation of FUS through Binding to Multiple Sites. *Cell*. **173** (3), 693–705.e622 (2018).
35. Chew, J. et al. Aberrant deposition of stress granule-resident proteins linked to C9orf72-associated TDP-43 proteinopathy. *Molecular Neurodegeneration*. **14** (1), 9 (2019).
36. Zhang, Y. J. et al. Poly(GR) impairs protein translation and stress granule dynamics in C9orf72-associated frontotemporal dementia and amyotrophic lateral sclerosis. *Nat Medicine*. **24** (8), 1136–1142 (2018).
37. Zhang, Y. J. et al. C9ORF72 poly(GA) aggregates sequester and impair HR23 and nucleocytoplasmic transport proteins. *Nature Neuroscience*. **19** (5), 668–677 (2016).
38. Zhang, Y. J. et al. Heterochromatin anomalies and double-stranded RNA accumulation underlie C9orf72 poly(PR) toxicity. *Science*. **363** (6428) (2019).
39. Beck, M., Hurt, E. The nuclear pore complex: understanding its function through structural insight. *Nature Reviews. Molecular Cell Biology*. **18** (2), 73–89 (2017).
40. Lin, D. H., Hoelz, A. The structure of the nuclear pore complex (an update). *Annual Review of Biochemistry*. **88**, 725–783 (2019).
41. Raices, M., D'Angelo, M. A. Nuclear pore complex composition: a new regulator of tissue-specific and developmental functions. *Nature Reviews. Molecular Cell Biology*. **13** (11), 687–699 (2012).
42. Kinoshita, Y., Kalir, T., Dottino, P., Kohtz, D. S. Nuclear distributions of NUP62 and NUP214 suggest architectural diversity and spatial patterning among nuclear pore complexes. *PLoS One*. **7** (4), e36137 (2012).
43. Ori, A. et al. Cell type-specific nuclear pores: a case in point for context-dependent stoichiometry of molecular machines. *Molecular Systems Biology*. **9**, 648 (2013).

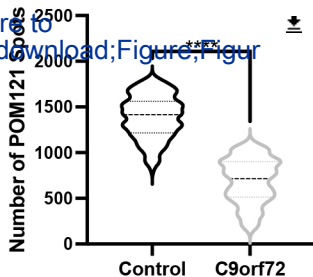
44. Rajoo, S., Vallotton, P., Onischenko, E., Weis, K. Stoichiometry and compositional plasticity of the yeast nuclear pore complex revealed by quantitative fluorescence microscopy. *Proceedings of the National Academy of Sciences of the United States of America*. **115** (17), E3969–E3977 (2018).
45. Li, C., Goryaynov, A., Yang, W. The selective permeability barrier in the nuclear pore complex. *Nucleus*. **7** (5), 430–446 (2016).
46. Raices, M., D'Angelo, M. A. Nuclear pore complexes and regulation of gene expression. *Current Opinion in Cell Biology*. **46**, 26–32 (2017).
47. Pascual-Garcia, P., Capelson, M. Nuclear pores in genome architecture and enhancer function. *Current Opinion in Cell Biology*. **58**, 126–133 (2019).
48. Schermelleh, L. et al. Subdiffraction multicolor imaging of the nuclear periphery with 3D structured illumination microscopy. *Science*. **320** (5881), 1332–1336 (2008).
49. Maglione, M., Sigrist, S. J. Seeing the forest tree by tree: super-resolution light microscopy meets the neurosciences. *Nature Neuroscience*. **16** (7), 790–797 (2013).
50. Thevathasan, J. V. et al. Nuclear pores as versatile reference standards for quantitative superresolution microscopy. *Nature Methods*. **16** (10), 1045–1053 (2019).
51. Wu, Y., Shroff, H. Faster, sharper, and deeper: structured illumination microscopy for biological imaging. *Nature Methods*. **15** (12), 1011–1019 (2018).
52. Hampoelz, B. et al. Pre-assembled nuclear pores insert into the nuclear envelope during early development. *Cell*. **166** (3), 664–678 (2016).
53. Hampoelz, B. et al. Nuclear pores assemble from nucleoporin condensates during oogenesis. *Cell*. **179** (3), 671–686.e617 (2019).
54. Agote-Aran, A. et al. Spatial control of nucleoporin condensation by fragile X-related proteins. *The EMBO Journal*. **39** (20), e104467 (2020).
55. Colombi, P., Webster, B. M., Fröhlich, F., Lusk, C. P. The transmission of nuclear pore complexes to daughter cells requires a cytoplasmic pool of Nsp1. *The Journal of Cell Biology*. **203** (2), 215–232 (2013).
56. Sivaguru, M. et al. Comparative performance of airyscan and structured illumination superresolution microscopy in the study of the surface texture and 3D shape of pollen. *Microscopy Research and Technique*. **81** (2), 101–114 (2018).
57. Löschberger, A., Franke, C., Krohne, G., van de Linde, S., Sauer, M. Correlative super-resolution fluorescence and electron microscopy of the nuclear pore complex with molecular resolution. *Journal of Cell Science*. **127** (Pt 20), 4351–4355 (2014).
58. Löschberger, A. et al. Super-resolution imaging visualizes the eightfold symmetry of gp210 proteins around the nuclear pore complex and resolves the central channel with nanometer resolution. *Journal of Cell Science*. **125** (Pt 3), 570–575 (2012).



A Figure 2_SIM Images

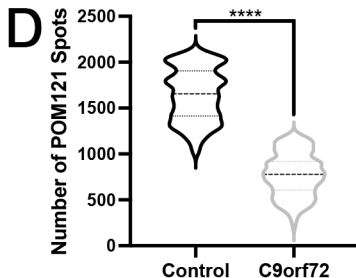
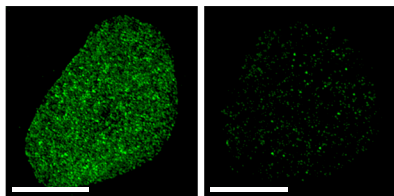


B [Click here to access/download;Figure;Figure](#)




C Human Motor Cortex

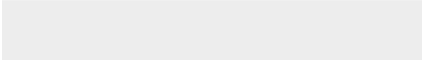

Control **C9orf72**



Culture Vessel	Volume of Lysis Buffer
12 well plate	0.5 mL per well
6 well plate	1 mL per well
10 cm dish	3 mL
T25 flask	2 mL



Click here to access/download
Table of Materials
Table of Materials-62789_R1.xls



Editorial comments:

1. Please take this opportunity to thoroughly proofread the manuscript to ensure that there are no spelling or grammar issues.

We have thoroughly read and edited the manuscript to remove any remaining spelling and grammar issues.

2. Please revise the text to avoid the use of any personal pronouns (e.g., "we", "you", "our" etc.).

Use of personal pronouns has been removed.

3. JoVE cannot publish manuscripts containing commercial language. This includes trademark symbols (™), registered symbols (®), and company names before an instrument or reagent. Please remove all commercial language from your manuscript and use generic terms instead. All commercial products should be sufficiently referenced in the Table of Materials. For example: Nuclei PURE Prep Nuclei Isolation Kit, Beckman SW 32 Ti rotor, Prolong Gold Antifade Reagent, Zeiss ELYRA S1

Company names have been removed when mentioned before an instrument or reagent. Commercial language has been removed when referencing all reagents. Reagents have been properly identified in the table of materials.

4. Please include an ethics statement before the numbered protocol steps, indicating that the protocol follows the guidelines of your institution's human research ethics committee.

This statement has been added accordingly.

5. Please remove the embedded Table from the manuscript. All tables should be uploaded separately to your Editorial Manager account in the form of an .xls or .xlsx file. Each table must be accompanied by a title and a description after the Representative Results of the manuscript text.

The table has now been removed and provided as a separate excel file. Further, all tables are now accompanied by a title and description after the representative results section.

6. Line 254: Please specify the parameters used for imaging (objective, magnification, filters, etc.).

We have now included this information for our representative results. However, as noted in the protocol, these parameters will vary depending on the imaging system and antibodies used.

7. Please ensure that the highlighted steps form a cohesive narrative with a logical flow from one highlighted step to the next. Please highlight complete sentences (not parts of sentences). Please ensure that the highlighted part of the step includes at least one action that is written in the imperative tense.

We have ensured that highlighted steps all contain at least one action and form a cohesive narrative.

8. As we are a methods journal, please revise the Discussion to explicitly cover the following in detail in 3-6 paragraphs with citations:

- a) Critical steps within the protocol
 - b) Any modifications and troubleshooting of the technique
 - c) Any limitations of the technique
 - d) The significance with respect to existing methods
 - e) Any future applications of the technique
9. Please do not use the &-sign or the word "and" when listing authors in the references.

The discussion covers critical steps within the protocol, modifications and troubleshooting of the technique, and limitations, significance, and applications of the technique.

Authors should be listed as last name author 1, initials author 1, last name author 2, initials author 2, etc. Title case and italicize journal titles and book titles. Do not use any abbreviations. Article titles should start with a capital letter and end with a period and should appear exactly as they were published in the original work, without any abbreviations or truncations.

References have been exported using the Jove Endnote style.

10. Figure 2: Please include scale bars in all the images of the panel.

Scale bars have been added to all images.

Reviewers' comments:

Reviewer #1:

Coyne and Rothstein report a protocol for isolating nuclei from neuron-differentiated induced pluripotent stem cells (iPSNs) and post-mortem human tissue for the purpose of immunostaining followed by imaging with super-resolution structured illumination microscopy (SIM).

The described protocol is of interest to the general nucleocytoplasmic transport community and wider because it enables for the resolution of individual nuclear pores on a purified nucleus by straightforward immunostaining of any nucleoporin.

Overall, the protocol is generally intelligible to a trained cell biologist or biochemist and suitable for publication.

However, there are a few instances where the authors make vague claims and a few instances where the authors use imprecise or incorrect language, which could be confusing to the reader. In line with the previous work from his lab, the senior author should ensure that the text is entirely precise and scientifically correct.

We thank the reviewer for their helpful comments to improve the clarity of our manuscript.

The authors should address the following points:

-- In the "SUMMARY", it should say "stem cell derived" instead of "stem cell derive".

We thank the reviewer for pointing out this spelling error.

-- Line 70: TEM, SEM, CryoEM are not mutually exclusive categories as CryoEM can be any EM technique that is performed under cryogenic conditions (most commonly transmission EM, TEM).

We appreciate the suggestion to provide clarification. Although TEM, SEM, and CryoEM are often discussed as separate methodologies, we agree with the reviewer that CryoEM is not necessarily a separate technique. We have therefore revised the text to just state TEM and SEM for simplicity.

-- Line 70: The authors state that "While electron microscopy (EM) techniques (TEM, SEM, CryoEM) are often used to evaluate the overall structure of NPCs, these methodologies do not allow for an accurate and reliable assessment of individual Nups themselves within NPCs or the nucleoplasm." How so? What do the authors mean by "reliable" and "accurate"? This is a vague and unscientific statement. The authors should precisely explain the advantages that SMI imaging affords over e.g. state of the art in situ cryoelectron-tomography.

We thank the reviewer for this suggestion and have now expanded our discussion on the comparison of EM vs fluorescence imaging (specifically SIM) for evaluating overall NPC ultrastructure vs individual Nup proteins within NPCs.

-- Line 75: "with a resolution that of approximately one human NPC" should be stated more precisely as "with a resolution that approaches the dimensions of a single human NPC".

We thank the reviewer for this suggestion.

-- The use of "sucrose gradient" to indicate the "sucrose gradient solution" throughout the protocol could be confusing, as "sucrose gradient", strictly speaking, indicates an actual gradient of sucrose concentrations. More broadly, the authors are performing a "sucrose cushion centrifugation" to isolate nuclei, so the use of the term "gradient" should be altogether avoided to prevent confusion with "sucrose gradient centrifugation" technique.

We thank the reviewer for pointing out the confusion that may be caused by the terminology. Sucrose gradient was the original terminology supplied by the manufacturer. However, this appears to have been updated in recently acquired kits. We agree that this might be confusing to those familiar with conventional sucrose gradients. As such, we have amended this accordingly and now use the term "sucrose cushion solution".

-- The process of isolating nuclei can result in washing out of the less stably attached nucleoporins from the NPC. The authors should discuss how this phenomenon may affect conclusions about NPC composition, as well as how this might affect reproducibility. It would be useful if the authors described any quality control steps that should be taken to ensure sample integrity (e.g. western-blot monitoring of nucleoporin levels at various steps).

We thank the reviewer for this suggestion as we have previously employed multiple "validation" strategies in our work (See Coyne et al (2020), Neuron). We have now added an expanded discussion of advantages and disadvantages of these quality control/validation techniques to our revised manuscript.

Reviewer #2:

Manuscript Summary:

The manuscript by Coyne and Rothstein describes a method for using SIM on isolated nuclei from in vitro derived neurons and human tissue to assess levels and distribution of nuclear pore complex (NPC) components (Nups). Overall, this is a well-written and clear description of a method that is very useful for the field. Nuclear pore alterations have been implicated in multiple

neurodegenerative pathologies, as well as in other human diseases and physiological states, and this method represents a high-resolution assay to accurately determine NPC and Nup distribution, levels, and integrity. Applying it would provide an initial characterization of possible NPC defects, and would shed light on mechanisms of a number of pathological states. I have a few relatively minor suggestions on improving clarity and impact of this protocol manuscript.

We thank the reviewer for their evaluation of our manuscript.

Major comments:

1. In the introduction, it would be helpful to mention/describe findings that linked actual NPC components or NPC integrity to neurodegenerative disease, either genetically or biochemically. It would underscore the need to accurately assess NPC components in the context of neuronal function.

We thank the reviewer for this suggestion and have amended our introduction accordingly.

2. Representative results: The authors could consider adding an example of quantification or analysis of images shown in Figure 2, to strengthen their message that their presented method accurately detects NPCs or individual Nups. Perhaps a plot of nuclear pore density obtained from single spots in such images and also a reference to a known density of NPCs? And/or alternatively, is it possible to show an example of this imaging in a neuron with a neurodegenerative phenotype, next to the shown WT nuclei? Since the title of the protocol is "Nuclei isolation and super resolution structured illumination microscopy for examining nucleoporin alterations in human neurodegeneration", it would be compelling to show such a "nucleoporin alterations in human neurodegeneration" and show that the method is able to distinguish it.

We thank the reviewer for this suggestion and have updated Figure 2 with an evaluation of POM121 spots in control and C9orf72 iPSNs and postmortem motor cortex. In agreement with our recent publication (Coyne et al (2020), Neuron) we show that this method can be used to reproducibly detect a reduction of POM121 from human neuronal NPCs in C9orf72 ALS/FTD.

Minor Concerns:

3. Abstract/Line 36: "Isolation of nuclei prior to SIM enables the visualization of individual Nup spots of the NPC..." - "Nup spots of the NPC" seems confusing. Unclear on what is meant by spots - signal from individual pores or individual proteins?

We appreciate the reviewer for pointing out the confusion generated by this statement. This has now been amended to "individual Nup proteins within the NPC".

4. Protocol: Line 91/Step1.2 "Add 50 μ L of 1 mg/mL collagen solution (diluted in 1X PBS) to the center of the circle" - please define circle, I am assuming it is the area that was outlined in the previous step?

We thank the reviewer for their suggestion and have added additional definition to these steps.

5. Line 180/Step 4.3 "Slowly add ~28 mL of lysate/sucrose gradient mix to the top of the sucrose gradient in the ultracentrifuge tube (from step 4.1)." - shouldn't it be 29 mL of lysate/sucrose gradient? 11 mL of prepared lysis buffer plus 18 mL of sucrose gradient. Steps 4.1-4.3 are a bit confusing so the exact number helps in referring to previous steps.

We agree with the reviewer that this is confusing. Indeed, it is 28 mL of lysate/sucrose gradient solution and not the full 29 mL. This is largely due to the viscosity of the sucrose gradient solution. As a result, the protocol is to add 28 mL of the full 29 mL for consistency across samples. This has now been noted and explained within the revised manuscript.

6. Line 249/Step 5.15 "Add 1 drop (~10 μ L) of Prolong Gold Antifade Reagent (without DAPI) to each slide and gently place high tolerance 18 mm x 18 mm square coverslips on each slide." - is there a sealing step after this? Are the coverslips in any way sealed to the slide?

We do not use a sealing step for our experiments. This has now been noted within the revised manuscript. It has also been noted that sealing can be done in certain situations (wet-mount media, prolonged storage).

7. Discussion: The authors could add a comment that the presented max projections in Figure 2 would not distinguish between NPC location vs. nucleoplasm location, and that alternative analysis of these SIM images would need to be used to look at specifically nuclear envelope-embedded NPCs. Furthermore, it would be beneficial to add a brief discussion of the types of specific Nup disruptions that have been reported in the context of neurodegenerative disease and that can be detected by this method.

We thank the reviewer for their helpful suggestion and have now edited the discussion accordingly. While the reviewer is correct that the images presented do represent maximum intensity projections of 3D reconstructed nuclei, we note that analysis is run on z stacks whereby individual z sections (or small stacks of z sections) are segmented independently in order to distinguish between spots associated with the nuclear envelope vs nucleoplasm.